# Stacking Interactions and DNA Intercalation

**ARTICLE** *in* THE JOURNAL OF PHYSICAL CHEMISTRY B · SEPTEMBER 2009

Impact Factor: 3.3 · DOI: 10.1021/jp905765c · Source: PubMed



**5 AUTHORS**, INCLUDING:

Valentino R. Cooper
Oak Ridge National Laboratory
**104** PUBLICATIONS **2,024** CITATIONS
SEE PROFILE

Bengt I. Lundqvist
Chalmers University of Technology
**177** PUBLICATIONS **13,365** CITATIONS
SEE PROFILE

# Stacking Interactions and DNA Intercalation

**Shen Li,*,†,‡ Valentino R. Cooper,†,§ T. Thonhauser,†,∥ Bengt I. Lundqvist,⊥ and David C. Langreth†**

*Department of Physics and Astronomy, Rutgers University, Piscataway, New Jersey 08854-8019, Fred Hutchinson Cancer Research Center, Seattle, Washington 98019, Oak Ridge National Laboratory, Oak Ridge, Tennessee 37831, Department of Physics, Wake Forest University, Winston-Salem, North Carolina 27109, and Department of Applied Physics, Chalmers University of Technology, SE-412 96 Göteborg, Sweden*

*Received: June 18, 2009*

The relationship between stacking interactions and the intercalation of proflavine and ellipticine within DNA is investigated using a nonempirical van der Waals density functional for the correlation energy. Our results, employing a binary stack model, highlight fundamental, qualitative differences between base-pair−base-pair interactions and that of the stacked intercalator−base-pair system. The most notable result is the paucity of torque, which so distinctively defines the twist of DNA. Surprisingly, this model, when combined with a constraint on the twist of the surrounding base-pair steps to match the observed unwinding of the sugar−phosphate backbone, was sufficient for explaining the experimentally observed proflavine intercalator configuration. Our extensive mapping of the potential energy surface of base-pair−intercalator interactions can provide valuable information for future nonempirical studies of DNA intercalation dynamics.



## 1. Introduction

Small ligands can interact with DNA by groove binding, intercalation, or nonspecific binding along the DNA exterior. DNA intercalation is the insertion of a small ligand or fragment between two adjacent base pairs in the DNA strand, forming stable sandwich-like structures. As a result, intercalation leads to significant perturbations to the DNA double helix. It opens a space between base pairs and unwinds the helical twist considerably.[1,2] The changes in the DNA structure disturb biological functions, such as transcription, replication and the DNA repair process. For that reason, inserting ligands, or intercalators, can be used as antitumor drugs and antiseptics. Due to their specificity for certain nucleic acid sequences, intercalators can also be used as nucleic acid dyes. Understanding their interactions with nucleic acids can make it possible to govern their behavior and therefore help design novel intercalating agents.

DNA intercalators are mostly polycyclic, aromatic, and planar. Their intercalation with DNA can be considered as a specific case of aromatic stacking interactions, where the dispersion energy plays an important role. There have been numerous experimental[3−10] and theoretical studies[11−18] carried out on intercalation systems. So far, most of the calculations are based on empirical or semiempirical methods and there are only a few *ab initio* studies.[16,19] The reason for this is that the size of the intercalation system is usually large and methods such as second-order Møller−Plesset perturbation theory (MP2) and coupled cluster (CCSD(T)) become impractical. The large size of the intercalation system can be reflected in two aspects. First, intercalator molecules usually have side chains of various sizes. To capture the binding properties, at least one intercalator and one DNA base pair have to be included in the calculation. Any complex smaller than that will not give the correct binding.[16] Typically, this gives systems too large for state-of-the-art coupled-cluster calculations at the basis set limit. Second, the intercalating process can also be affected by factors such as water in the environment, twisting of the DNA backbone, and entropic effects. From these aspects, theoretical studies based on empirical methods have their advantages. Intercalator and DNA base pairs, as well as water molecules and the DNA backbone, can be included without introducing too much computational cost. Thermodynamic processes can be simulated by computational experiments, e.g., via molecular dynamics.[20] However, the accuracy of these calculations depends on the empirical potentials, which are highly system dependent. To gain more reliable information for the DNA intercalation process, an efficient higher level computational technique is desirable.

For many years, density functional theory (DFT) has been widely accepted as a useful tool for understanding and predicting the electronic properties of materials. Compared to quantum chemical methods such as MP2 or CCSD(T), standard DFT methods are often a better choice for large-sized systems because of the computational cost. It is efficient, and for both dense matter as well as isolated molecules, it typically has sufficient accuracy. Nevertheless, for van der Waals (vdW) complexes and sparse matter, where the dispersion energy is important, standard density functionals are often inadequate. To remedy the situation, a van der Waals density functional (vdW-DF) has been developed, which can approximately treat long-range dispersion interactions with no empirical input.[21,22] VdW-DF and variants have been applied to a number of vdW systems from relatively simple complexes[21−29] to large systems.[30−39] Reviews also exist.[40,41] In particular, it has been applied to the prediction of the DNA twist.[42,43] To complement these studies, we have calculated the interaction energies of the adenine−thymine stack and the uracil dimer for the S22 geometries of Jurecka et al.,[44] with further optimization of the rise to arrive

* Corresponding author. E-mail: sl2@fhcrc.org.
† Rutgers University.
‡ Fred Hutchinson Cancer Research Center.
§ Oak Ridge National Laboratory.
∥ Wake Forest University.
⊥ Chalmers University of Technology.

10.1021/jp905765c CCC: $40.75 
Published on Web 07/14/2009

**TABLE 1: Stacking Energies (kcal/mol)**

| | vdW-DF | CCSD(T) |
|---|---|---|
| adenine−thymine stack | −10.60 | −12.23 |
| uracil dimer stack | −9.41 | −10.12 |

closer to the vdW-DF minimum. In Table 1, we compare these vdW-DF values with those calculated via state-of-the-art coupled-cluster methods.[44] An important recent development is that of an efficient algorithm[37] which allows vdW-DF to be applied to large systems with virtually the same efficiency as standard generalized gradient methods. Unfortunately, this development was not available at the time that the present calculations were performed; however, its use on a rather large system was recently illustrated in ref 37.

In this paper, we studied the intercalation systems of proflavine and ellipticine using vdW-DF. Lacking side chains, proflavine has the simplest form among the intercalators. Several crystallographic studies on proflavine-intercalated DNA have been reported.[3−5] Theoretically, a number of calculations based on empirical methods have been carried out.[11−15] Starting from the crystal structures obtained from experiments, optimized configurations and the components of the binding energy were predicted.

Ellipticine is another simple intercalator. It is a natural plant product which exhibits powerful antitumor and anti-HIV activities.[45] Řeha et al. have reported results from calculations using MP2, dispersion corrected density functional tight-binding (DFTB-D) methods, and empirical force fields.[16] They studied the smallest possible complete model, which is represented by one intercalator stacked above one DNA base pair. Using three different levels of calculation, they investigated the vertical separation dependence and twist angle dependence of the stacking energy and compared the performance of the different methods.

In this paper, we adopt the same intercalation model as Řeha et al.[16] Since this is the first application of vdW-DF to DNA intercalation, we limit our calculations to the smallest intercalation model, instead of studying the complex, real-life process. Here, we treat intercalation simply as a stacking problem and concentrate on the role of the interaction between the intercalator and the neighboring base pairs in determining the optimum configuration. Interactions with the phosphodiester strands, water molecules, or counterions in the environment are not considered. The process whereby an intercalator goes from a solvated state in the environment to its intercalated configuration involves a number of energetic and entropic contributions which are not studied here. Our results, however, can give insight into base-pair−intercalator interactions and the role they play in determining final intercalating configurations.

Our studies on ellipticine focus on testing our method against existing MP2 results. More complete calculations were performed on proflavine to explore the optimized energy surface in greater detail, including a comparison with experiment.

## 2. Computational Details

VdW-DF can be implemented in two different ways: (i) Self-consistently, where the exchange-correlation potential corresponding to the nonlocal vdW-DF is included as part of the Kohn−Sham potential and the charge density used to evaluate the energy is fully self-consistent, and (ii) non-self-consistently, where the nonlocal correlation energy (i.e., the vdW-DF correction) is evaluated as a postprocessing perturbation, using a charge density obtained from self-consistent calculations with

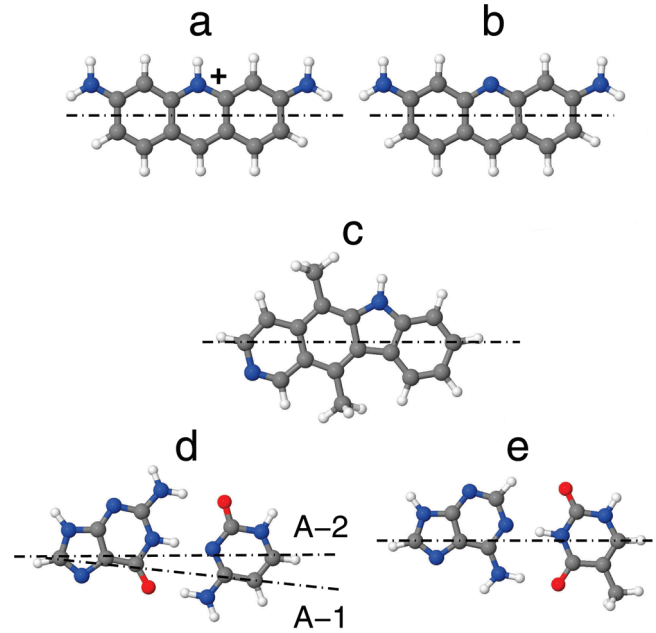


**Figure 1.** Configurations of (a) proflavine, (b) neutral proflavine, (c) ellipticine, (d) C:G base pair, and (e) T:A base pair. Atoms are colored using the CPK convention (nitrogen, blue; oxygen, red; carbon, black; hydrogen, white). The dashed lines indicate the direction of the main axes.

either the Perdew−Burke−Ernzerhof (PBE)[46] or revised PBE (revPBE) functionals.[47] Previous studies[22,26] have demonstrated that the self-consistent and non-self-consistent implementations lead to nearly indistinguishable results for interaction energies. This occurs because the van der Waals interaction is so weak and diffuse that it does not substantially change the electronic charge distribution. In this paper, all calculations are done with non-self-consistent vdW-DF.

Here, we implemented vdW-DF within the code PARSEC,[48] which is based on self-consistently solving the Kohn−Sham equations on a uniform, real-space grid. This method has a number of advantages. For example, one can study vdW complexes with dipole moments or net charges more efficiently, since no supercell geometry or periodic boundary conditions are involved. This is especially valuable for DNA intercalators. Furthermore, compared with localized basis methods, the choice of basis set is not an issue; one simply decreases the grid spacing until convergence is obtained. Here, we found that an accuracy of 0.02 kcal/mol could be obtained with a grid spacing of 0.3 Bohr. We used Troullier−Martins pseudopotentials.[49] The systems were placed at the center of a spherical domain large enough to ensure that all the wave functions vanish smoothly at the boundary. For these calculations, we used a spherical radius of 22 Bohr.

## 3. Results and Discussion

**3.1. Isolated Intercalators and DNA Base Pairs.** We first optimized the ground-state structure of the intercalator and DNA base pairs using PBE. The configurations are shown in Figure 1. Since proflavine is positively charged, we also studied its hypothetical variant, neutral proflavine, to investigate the electrostatic effects on intercalation.

The direction of the main axes of the intercalators and base pairs is plotted as dashed lines in Figure 1. We define the center of the intercalator/base pair as follows: For proflavine, the center of the molecule is the center of the middle aromatic ring. For ellipticine, the center is taken to be the mass center in order to

**TABLE 2: Ellipticine and Proflavine Dipole Moments (Debye) and Polarizabilities (Å$^3$)**

| | Ellipticine | |
|---|---|---|
| | dipole | polarizability |
| this work | 4.2 | 36.9 |
| Hartree−Fock[16] | 3.9 | 27.3 |
| | Proflavine | |
| charge | dipole | polarizability |
| 0 | 0.6 | 34.3 |
| +\|e\| | 2.7 | 33.7 |

be consistent with previous studies.[16] For the cytosine−guanine (C:G) pair, we use the line A-1 (see Figure 1d) and the mass center to define the main axis and the base-pair center when stacked with ellipticine, again, for consistency with previous studies.[16] When stacked with proflavine, the standard axis intersecting C6−C8[50] (A-2 in Figure 1d) is the main axis and the C6−C8 midpoint is the center. In the case of the thymine−adenine (T:A) pair, the center is again set at the C6−C8 midpoint. Generally, we follow the conventions of the Nucleic Acid Database[50] in labeling base pairs and base-pair steps.

We studied the distribution of proflavine's excess charge. This is the difference between the electronic charge distribution of the charged proflavine molecule and that of the combination of a neutral proflavine molecule and an isolated H atom located at the top of the middle aromatic ring. We found that the resulting positive unit charge is delocalized throughout the molecular plane, which is consistent with previous observations on other charged intercalators.[16] Dividing the molecular plane into three areas—the middle ring area and the areas to the left and to the right—we find that only ∼50% positive charge is located in the middle area with most of this charge located at the top of the ring (Figure 1a), i.e., near the N−H bond. The remaining positive charge is symmetrically distributed in the left and right rings.

We have calculated the dipole moments and polarizabilities of ellipticine and of both the charged and neutral proflavine (Table 2). From our calculations, both ellipticine and proflavine (charged and neutral) have large polarizabilities. This suggests that the dispersion energy should be important for intercalation. Since the charged and neutral proflavine have similar polarizabilities, the dispersion energy should make a similar contribution to the binding energy of either one to a base pair.

In the sections that follow, we study the interaction energy of the intercalator−base-pair complex. The intercalator and DNA base pair are stacked in parallel planes in such a way that the main axes are parallel and the centers are positioned above each other. We vary the vertical separation, twist angle, and horizontal translation. The vertical separation is the vertical distance ($z$ direction) between intercalator and base-pair centers. The twist angle is the angle between the main axes of the intercalator and the base pair. The alignment of the two main axes leads to two different configurations with 180° difference in the twist angle. We arbitrarily choose one as the parallel configuration while the other as the antiparallel case. Finally, the horizontal translation is the horizontal distance (in the $xy$ plane) between intercalator and base-pair centers, which includes both shift and slide in standard DNA parlance.[51]

**3.2. Ellipticine−C:G Complex.** We studied the ellipticine−C:G complex by varying the vertical separation and the twist angle, respectively. Figure 2 shows the vertical separation dependence of the interaction energy. The MP2 and DFTB-D

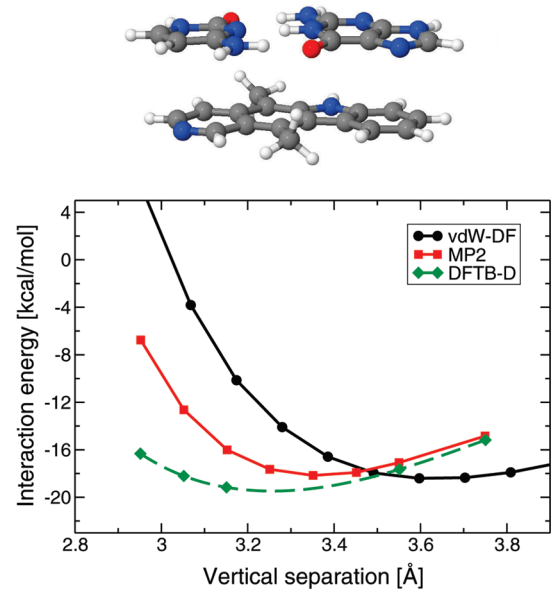


**Figure 2.** Interaction energy as a function of the vertical separation for the ellipticine−C:G complex. The ellipticine molecule is aligned with the A-1 axis on C:G (Figure 1), with the centers of mass of the two species vertically over each other.

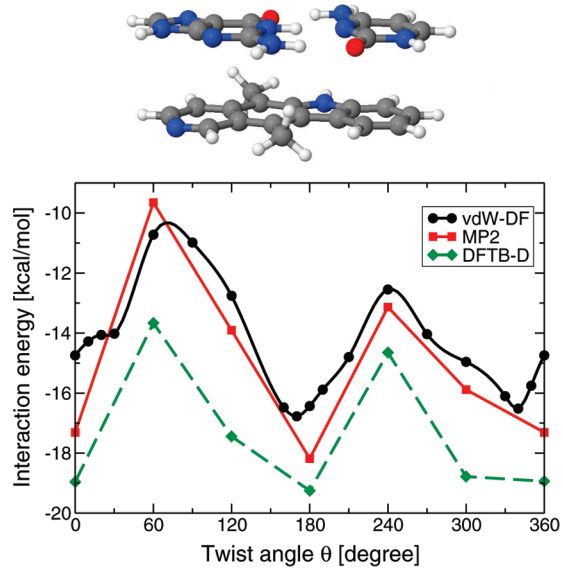


**Figure 3.** Interaction energy as a function of the twist angle $\theta$ for the ellipticine−G:C complex, where a positive $\theta$ implies a right-handed twist. The vertical separation is fixed at 3.4 Å. The ball-and-stick model shows the configuration with zero twist angle $\theta$.

results from Řeha et al.[16] are also included. Here, we find an optimum separation of 3.6 Å with a corresponding energy of −18.4 kcal/mol. MP2 results give ∼3.4 Å and ∼ −18.2 kcal/mol. The difference between our results and results from MP2 is ∼6% for the optimum separation and ∼1% for the corresponding energy.

Figure 3 shows the twist angle dependence of the interaction energy. The ball-and-stick model gives the configuration with zero twist angle. The vertical separation is fixed at 3.4 Å to be consistent with the MP2 calculations.[16] From the plot, we can see that there are two minima in the energy curve, which correspond to configurations where the main axis of the intercalator is either nearly parallel (340°) or nearly antiparallel (170°) to the main axis of the base pair. The energy difference between the two minima is ∼0.2 kcal/mol. Our calculations give an optimum twist angle of 170° with an energy of −16.8 kcal/

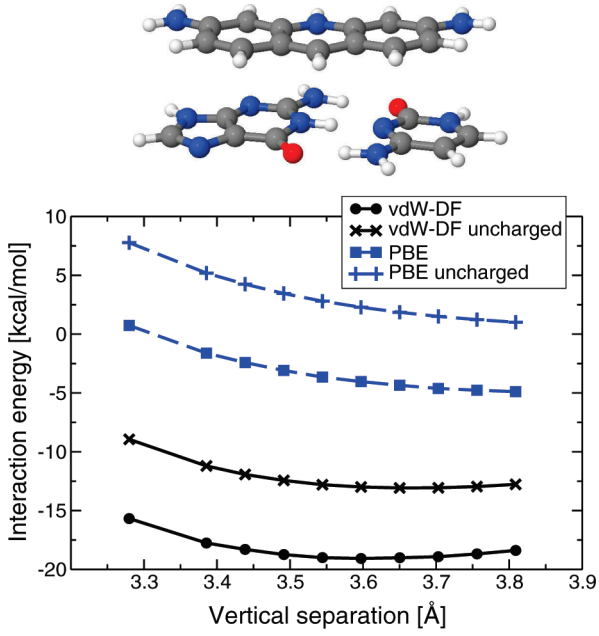


**Figure 4.** Interaction energy as a function of the vertical separation for the proflavine−C:G complex. The proflavine is aligned with the C6−C8 axis on C:G (direction of A-2 in Figure 1d), with its center over the midpoint of C6−C8.

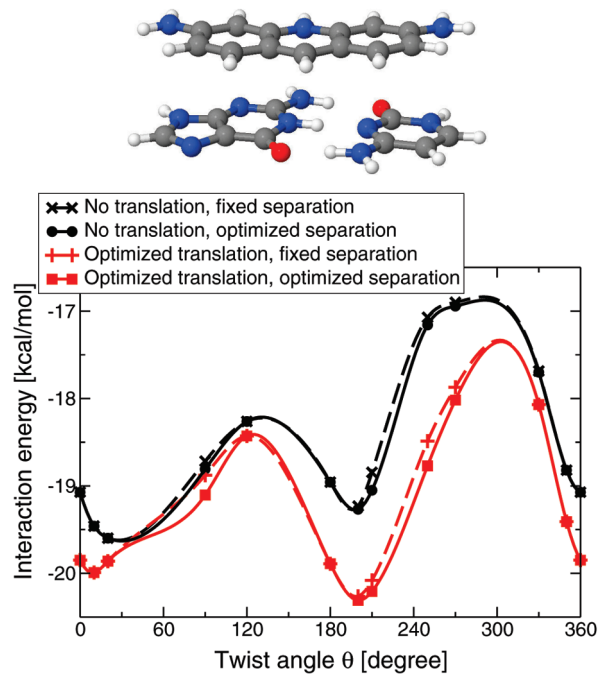


**Figure 5.** Interaction energy as a function of the twist angle $\theta$ for the proflavine−C:G complex, with a right-handed twist corresponding to a positive $\theta$. The ball-and-stick model shows the configuration for $\theta = 0$, as in Figure 4. For the cases of fixed separation, the vertical separation is fixed at 3.6 Å.

mol, whereas MP2 gives a rough minimum around 180° and −18.2 kcal/mol, respectively. From Figure 3, one can see that vdW-DF successfully reproduces all of the features shown in the MP2 curve, and that it gives much better agreement with the MP2 results than with the DFTB-D ones.

**3.3. Proflavine−C:G Complex.** We studied both charged and neutral proflavine by varying the vertical separation between proflavine and the C:G pair. The interaction energy vs vertical separation is plotted in Figure 4. We also plot the results from PBE calculations. Our results show that vdW-DF gives much stronger binding than PBE whose energy curve is shallow, with no minimum within the investigated range. This indicates that the dispersion energy, which is not included in PBE, is very important for intercalation. Charged proflavine is also shown to have stronger binding than neutral proflavine. However, the binding energy *difference* is similar in vdW-DF and PBE calculations, suggesting that this difference is due to self-consistent electrostatics, rather than dispersion. The similarity of the polarizabilities of the two proflavine forms also suggests that the differences in the dispersion interactions are small, thus strengthening the above conclusion.

For charged proflavine, we studied the twist angle dependence of the interaction energy. The configuration of the complex and the energy curves are shown in Figure 5. The proflavine rotates in a right-handed way. We considered the following situations for each twist angle: (i) vertical separation of 3.6 Å and horizontal translation of zero, (ii) vertical separation optimized and horizontal translation of zero, (iii) vertical separation of 3.6 Å and horizontal translation optimized, and (iv) vertical separation and horizontal translation both optimized.

From the plot, we can see that there are two minima in all of the energy curves. One corresponds to the configuration where the main axis of proflavine is nearly parallel (∼20°) to the main axis of the C:G pair. The other corresponds to the nearly antiparallel (∼200°) situation. The energy difference is less than 0.5 kcal/mol for all cases. If both vertical separation and horizontal translation are fixed, the optimum angle is 20°. Optimization changes the optimum angle from 20 to 200°. The corresponding minimum energy is −20.3 kcal/mol. From our calculations, optimized separation and horizontal translation do not change very much with the change of the twist angle. The change is within 1 Å for separation and 2.5 Å for the magnitude of the horizontal translation.

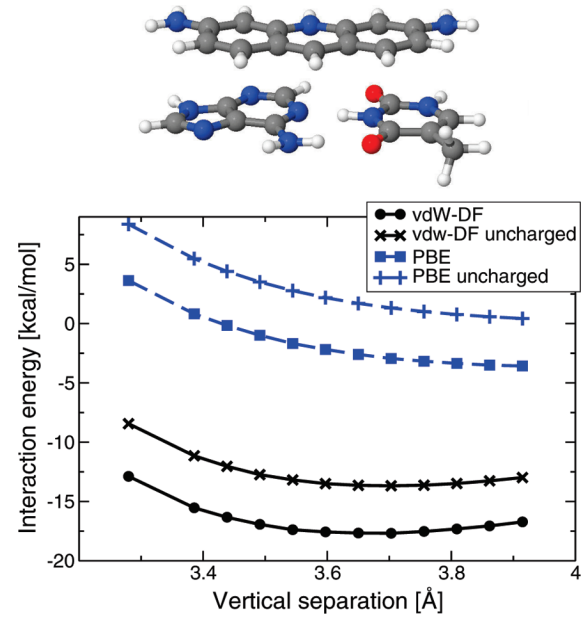


**Figure 6.** Interaction energy as a function of the vertical separation for the proflavine−T:A complex.

**3.4. Proflavine−T:A Complex.** The interaction energy between proflavine and the base pair T:A is studied in the same way as proflavine with C:G. The vertical separation dependence of the interaction energy is plotted in Figure 6, and the twist angle dependence of the interaction energy is plotted in Figure 7.

From Figure 6, we can see that, similar to the proflavine−C:G complex, the vdW-DF gives much stronger binding than PBE

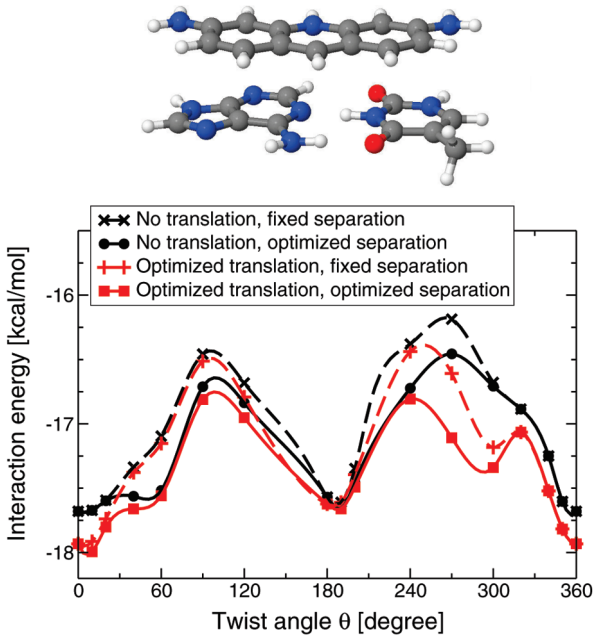


**Figure 7.** Interaction energy as a function of the twist angle $\theta$ for the proflavine−T:A complex, with a right-handed twist corresponding to a positive $\theta$. The ball-and-stick model shows the configuration for $\theta = 0$, as in Figure 6. For the cases of fixed separation, the vertical separation is fixed at 3.7 Å.

and the difference between charged and neutral proflavine is purely electrostatic.

In Figure 7, for all four energy curves, the interaction energy is minimized only if proflavine is parallel (∼0°) or antiparallel (∼180°) to the T:A pair. The energy difference between the two minima is less than 0.5 kcal/mol. Optimizing separation and horizontal translation does not introduce big changes in the energy curve. The optimum twist angle is 10°, and the corresponding energy is −18.0 kcal/mol. Compared with the minimum energy of the proflavine−C:G complex (−20.3 kcal/mol), proflavine seems to prefer binding with a C:G pair. It should be noted that there are some rapid variations in the energy curve around 40 and 320°. These correspond to the steric clash between H atoms in proflavine and the methyl group of the T:A pair.

**3.5. Intercalator−BP Interaction vs BP−BP Interaction.** We compared the intercalator−base-pair interaction with the base-pair−base-pair interaction. The angular dependence of ellipticine and proflavine interacting with a base pair (BP) (see Figures 3 and 5) shows a dramatic difference from that of the interaction between BPs with each other. For illustration, in Figure 8, we show the interaction of GC:GC and CG:CG from the calculations of Cooper et al.[42,52] We also plot the interaction of proflavine−C:G near the lowest local minima corresponding to an antiparallel twist angle of $\theta - 180°$ for comparison. We find that, for the case of intercalator−BP, the interaction energy is stronger overall and the change in the interaction energy with the change of twist angle is usually smaller. That makes the energy vs twist angle curve of intercalator−BP deeper and flatter, as shown in Figure 8. It implies that intercalation is energetically preferred. However, torque from the intercalator is not likely to have as strong an effect on determining the twist of adjacent base pairs as base pairs would have on each other in a sequence without intercalation.

In addition, the BP−BP stacking interaction typically has two minima at both positive *and* negative small angles, showing a double-well around zero-degree twist angle in the angular

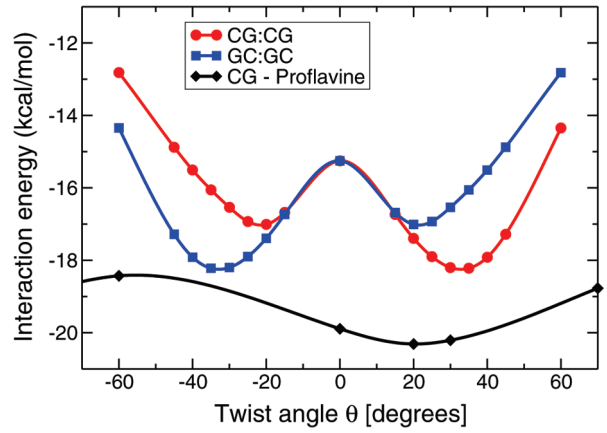


**Figure 8.** Angular dependence of the interaction energy at small angle for two base-pair sequences and a proflavine−C:G sequence. In the latter case, the twist, for the purposes of this figure *only*, is defined as $\theta - 180°$, where $\theta$ is the abscissa of Figure 5.

dependence of the interaction energy curve. One such minimum generally occurs in the range between 30 and 40° and the other in the range between −40 and −30°.[42] The positive minimum corresponds to a right-handed twist of the particular sequence, while the minimum at negative angle corresponds to a right-handed twist of the reverse sequence. This is shown by the blue square points and red circular points for the GC:GC sequence and the CG:CG sequence, respectively, in Figure 8.

However, the feature of double-well around small angle does not appear in the two intercalators we study here, where there is only a single minimum at "small" angle. *Small* is put in quotes above because it could refer to either $\theta$ (as defined as the abscissa in Figures 3 and 5) being small or alternatively ($\theta - 180°$) being small. The fact that there is a single small angle minimum seems to play a role in providing some stability to the small angle intercalator configuration, which, unlike the base pairs, does not have the help of the phosphodiester strands to select a stable minimum.

**3.6. Proflavine Intercalated into the CG:CG Step.** We compared our calculations with experimental results.[4] According to the crystallographic studies, the CG:CG step partly unwinds, allowing proflavine to intercalate between the C:G and G:C pairs to form a sandwich-like structure, as shown in Figure 9a. Due to proflavine's symmetry, the stacking configuration of proflavine with an upper G:C (part II) should be exactly the same as proflavine with a lower C:G (part I). This sameness can be easily visualized by turning part II upside down to compare with part I. We extracted the twist angle for parts I and II from the experimentally determined[4] atomic coordinates. To be consistent, we used the same definition of zero twist angle, as shown in Figure 5. We also turned part II upside down for extracting the angle. We expected that the twist angle for the two parts would be around 200°, as shown in Figure 5. However, we found that the twist angle is 198° for part I and 178° for part II. The inconsistency in the twist angle for the two might come from the effect of the phosphodiester backbone in influencing the twist between the G:C and C:G pairs which, according to experiment,[4] is 16°. In intercalation, the backbone may resist the rather severe winding of the base pairs. This is further supported by the shallowness of the minimum in the C:G−proflavine curve in Figure 8, which, as indicated above, shows that torque from the intercalator does not have a strong effect on the twisting of adjacent base pairs.

We artificially introduced the twisting effect of the DNA backbone by adding interaction energies of two parts, G:C−pro-

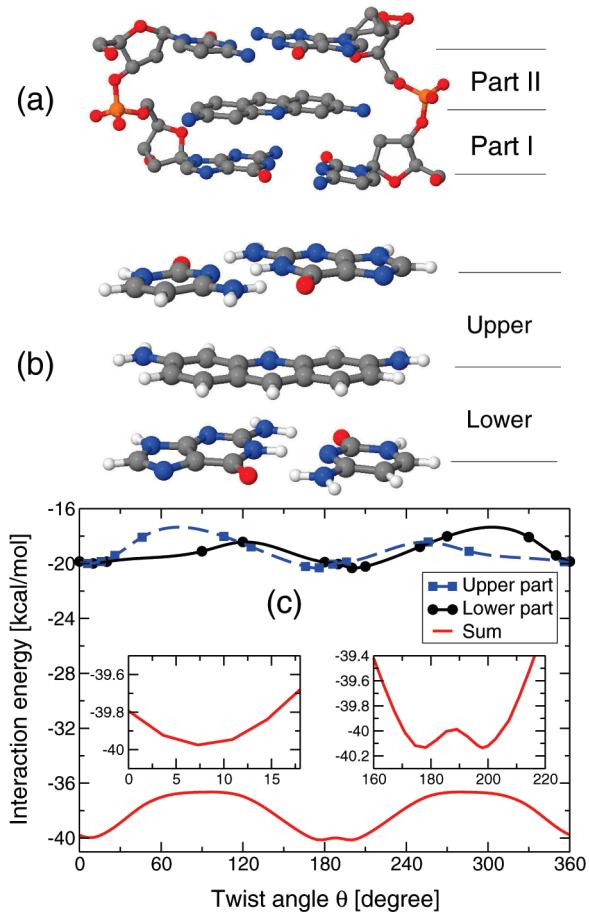


**Figure 9.** (a) Configuration observed in experiment. NDB ID: ddb034. H atoms are not shown. (b) $\theta = 0$ configuration in our calculations. Initially, the proflavine is aligned with the lower C:G axis C6−C8 (direction of A-2 in Figure 1d). The upper base pair (G:C) is fixed at a 16° right-handed twist with respect to the lower base pair (C:G). (c) The interaction energy as a function of the right-handed twist angle $\theta$ between the proflavine and the lower base pair (C:G). The energy curves for the upper and lower parts are from the optimized energy curve (solid red curve with square points) in Figure 5 appropriately shifted (see text). The red curve without symbols is the sum of the blue dashed and black solid curves and hence represents the total interaction energy.

flavine and proflavine−C:G, together, while keeping the right-handed twist angle of the CG:CG step at its experimental value of +16°. The twist angle vs interaction energy curves are plotted in Figure 9c. The black solid curve is simply a transcription of the solid red curve with square points of Figure 5, representing the interaction between the proflavine and the lower base pair. The blue dashed curve is the result of letting $\theta \rightarrow -\theta$ in a periodic extension of the solid red curve with square points in Figure 5 followed by a 16° shift. Letting $\theta \rightarrow -\theta$ is to account for the left-handed rotation of proflavine with respect to the upper base pair. The 16° shift is to account for the assumed fixed twist between the upper base pair and the bottom one. Thus, the blue dashed curve represents the interaction energy between the proflavine and the upper base pair as a function of the twist $\theta$ of the proflavine with respect to the lower base pair. The red curve without symbols is the sum of the other two curves, and represents the net interaction energy between the proflavine and the fixed base-pair configuration. The ball-and-stick model (Figure 9b) shows the fixed base-pair configuration, with the proflavine at an angle of $\theta = 0$ as in Figure 5.

From the red curve (solid line), one can clearly see that there are two optimum twist angles, 178 and 198°, which means that the twist angle between proflavine and the lower base pair (C:G) can be either one. If the twist angle with the lower pair is 178°, since we fixed the twist angle of the (CG:CG) step, then the angle between proflavine and the upper base pair (G:C) would be 198°. Otherwise, if the twist angle with the lower base pair (C:G) is 198°, then the angle with the upper base pair (G:C) would be 178°. Considering the fact that proflavine is symmetric, i.e., there is no difference between the upper and lower parts, our results are exactly consistent with the experimental results.

We also noticed that there is another minimum around 7° with an interaction energy higher than the global minimum by 0.2 kcal/mol. Although the energy difference is small, this minimum is not observed in the experiment. This could be because the observed configuration is further stabilized relative to the unobserved one by interactions not included in the stacking model. A 10% effect of this sort on the interaction energy as a function of angle could change the tiny energy splitting between the two minima by an order of magnitude. A similar effect on the splitting could be produced by the likely 10% error in the calculations. If the near degeneracy still remains after the above considerations are accounted for, then the statistical mechanical phase space (involving all relevant degrees of freedom, not just the optimized curves shown) would have to be much larger for the observed configuration than the other one. This seems unlikely.

Using our interaction energy while fixing the DNA twist angle, we successfully reproduced the experimental results for the intercalating configuration of proflavine. Our results suggest that the final intercalating configuration cannot be uniquely determined by the interaction energy between intercalator and base pair; the twist of the DNA backbone will also affect the configuration. Since intercalation opens a space between adjacent DNA base pairs, the DNA backbone is heavily stretched. Thus, the twist of the DNA backbone is not flexible anymore, and it may be an obstacle to the twisting of the intercalation system.

## 4. Conclusion

We calculated the interaction energy of ellipticine−C:G, proflavine−C:G, and proflavine−T:A complexes using DFT utilizing the van der Waals exchange-correlation functional (vdW-DF).[21] Our results show that the configurations of these intercalating systems are stabilized only when the main axis of the intercalator is nearly aligned with the main axis of the base pair. For charged proflavine, this may be due to the tendency to maximize the induced Coulomb attraction, while, for neutral ellipticine, it may be due to steric clashes involving the intercalator's side methyl groups, which can occur in more twisted configurations. In either case, the feature of *two* minima at small angles observed in base-pair−base-pair interactions is not observed in intercalator−base-pair interactions. Another interesting feature is the comparison between maximum interaction energy strength and maximum torque strength. Although the interaction energy strength between these intercalators and a base pair is larger than that between two base pairs, its range of variation with respect to angle is smaller (e.g., see Figure 5). So also is the average magnitude of its rate of variation with respect to angle. This means that the torque from the intercalator does not have as strong an effect on determining the twist of adjacent base pairs as base pairs would have on each other.[42]

Our results for the ellipticine−C:G complex give good agreement with the results from quantum-chemical calculations. For proflavine, we used the calculated interaction energy and

torque between base pair and intercalator, and by constraining the twist of the base pairs which sandwich it to the experimental value, we successfully reproduced the experimental configuration, with the correct twist of the intercalator. Our results show that the stacking interaction between base pair and intercalator cannot uniquely determine the final intercalating configuration, and that the twist of the DNA backbone will also affect the intercalation. Better knowledge of the structures and mechanisms for the intercalation of such drug molecules will undoubtedly play an important role in drug design and understanding their action. The good agreement between our results and the previous experimental and theoretical studies suggests that vdW-DF is a useful tool for studying similar weakly interacting systems. It is especially valuable for larger systems for which alternative nonempirical methods are prohibitively expensive.

**Acknowledgment.** We thank W. K. Olson for valuable discussions. This work was supported in part by NSF-DMR-0456937 and NSF-DMR-0801343. Work at ORNL was supported by D.O.E., Division of Materials Sciences and Engineering.

**Supporting Information Available:** Complete figures of the twist angle dependence of the intercalation for proflavine−C:G and proflavine−T:A. Also complete refs 40, 41, and 51. This material is available free of charge via the Internet at http://pubs.acs.org.



## References and Notes

(1) Lerman, L. S. *J. Mol. Biol.* **1961**, *3*, 18.
(2) Bond, P. J.; Langridge, R.; Jennette, K. W.; Lippard, S. J. *Proc. Natl. Acad. Sci. U.S.A.* **1975**, *72*, 5825.
(3) Shieh, H. S.; Berman, H. M.; Dabrow, M.; Neidle, S. *Nucleic Acids Res.* **1980**, *8*, 85.
(4) Schneider, B.; Ginell, S. L.; Berman, H. M. *Biophys. J.* **1992**, *63*, 1572.
(5) Westhof, E.; Hosur, M. V.; Sundaralingam, M. *Biochemistry* **1988**, *27*, 5742.
(6) Tang, P.; Juang, C. L.; Harbison, G. S. *Science* **1990**, *249*, 70.
(7) Aslanoglu, M. *Anal. Sci.* **2006**, *22*, 439.
(8) Alonso, A.; Almendral, M. J.; Curto, Y.; Criado, J. J.; Rodríguez, E.; Manzano, J. L. *Anal. Biochem.* **2006**, *355*, 157.
(9) Canals, A.; Purciolas, M.; Aymamí, J.; Coll, M. *Acta Crystallogr.* **2005**, *D 61*, 1009.
(10) Berge, T.; Jenkins, N. S.; Hopkirk, R. B.; Waring, M. J.; Edwardson, J. M.; Herderson, R. M. *Nucleic Acids Res.* **2002**, *30*, 2980.
(11) Neidle, S.; Pearl, L. H.; Herzyk, P.; Berman, H. M. *Nucleic Acids Res.* **1988**, *16*, 8999.
(12) Kim, K. S.; Corongiu, G.; Clementi, E. *J. Biomol. Struct. Dyn.* **1983**, *1*, 263.
(13) Mezei, M.; Beveridge, D. L.; Berman, H. M.; Goodfellow, J. M.; Finney, J. L.; Neidle, S. *J. Biomol. Struct. Dyn.* **1983**, *1*, 287.
(14) Swaminathan, S.; Beveridge, D. L.; Berman, H. M. *J. Physiol. Chem.* **1990**, *92*, 4660.
(15) Nuss, M. E.; Marsh, F. J.; Kollman, P. A. *J. Am. Chem. Soc.* **1979**, *101*, 825.
(16) Řeha, D.; Kabeláč, M.; Ryjáček, F.; Šponer, J.; Šponer, J. E.; Elstner, M.; Suhai, S.; Hobza, P. *J. Am. Chem. Soc.* **2002**, *124*, 3366.
(17) Trieb, M.; Rauch, C.; Wibowo, F. R.; Wellenzohn, B.; Liedl, K. *Nucleic Acids Res.* **2004**, *32*, 4696.
(18) Kubař, T.; Hanus, M.; Ryjáček, F.; and Hobza, P. *Chem.—Eur. J.* **2006**, *12*, 280.
(19) Langner, K. M.; Kedzierski, P.; Sokalski, W. A.; Leszczynski, J. *J. Phys. Chem. B* **2006**, *110*, 9720.
(20) Elcock, A. H.; Rodger, A.; Richards, W. G. *Biopolymers* **1996**, *39*, 309.
(21) Dion, M.; Rydberg, H.; Schröder, E.; Langreth, D. C.; Lundqvist, B. I. *Phys. Rev. Lett.* **2005**, *95*, 109902.
(22) Thonhauser, T.; Cooper, V. R.; Li, S.; Puzder, A.; Hyldgard, P.; Langreth, D. C. *Phys. Rev. B* **2007**, *76*, 125112.
(23) Puzder, A.; Dion, M.; Langreth, D. C. *J. Chem. Phys.* **2006**, *124*, 164105.
(24) Thonhauser, T.; Puzder, A.; Langreth, D. C. *J. Chem. Phys.* **2006**, *124*, 164106.
(25) Hooper, J.; Cooper, V. R.; Thonhauser, T.; Romero, N. A.; Zerilli, F.; Langreth, D. C. *ChemPhysChem* **2008**, *9*, 891.
(26) Li, S.; Cooper, V. R.; Thonhauser, T.; Puzder, A.; Langreth, D. C. *J. Phys. Chem. A* **2008**, *112*, 9031.
(27) Vydrov, O. A.; Wu, Q.; Van Voorhis, T. *J. Chem. Phys.* **2008**, *129*, 014106.
(28) Vydrov, O. A.; Van Voorhis, T. *J. Chem. Phys.* **2009**, *130*, 104105.
(29) Gulans, A.; Puska, M. J.; Nieminen, R. M. *Phys. Rev. B* **2009**, *79*, 201105(R).
(30) Chakarova-Käck, S. D.; Schröder, E.; Lundqvist, B. I.; Langreth, D. C. *Phys. Rev. Lett.* **2006**, *96*, 146107.
(31) Kleis, J.; Lundqvist, B. I.; Langreth, D. C.; Schröder, E. *Phys. Rev. B* **2007**, *76*, 100201(R).
(32) Johnston, K.; Kleis, J.; Lundqvist, B. I.; Nieminen, R. M. *Phys. Rev. B* **2008**, *77*, 121404. Erratum: *Phys. Rev. B* **2008**, *77*, 209904.
(33) Nabok, D.; Pusching, P.; Ambrosch-Draxl, C. *Phys. Rev. B* **2008**, *77*, 245316.
(34) Sony, P.; Pusching, P.; Nabok, D.; Ambrosch-Draxl, C. *Phys. Rev. Lett.* **2008**, *99*, 176401.
(35) Yanagisawa, S.; Lee, K.; Morikawa, Y. *J. Chem. Phys.* **2008**, *128*, 244704.
(36) Kleis, J.; Schröder, E.; Hyldgaard, P. *Phys. Rev. B* **2008**, *77*, 205422.
(37) Román-Pérez, G. Soler, J. arXiv:0812.0244, 2008.
(38) Kong, L.; Cooper, V. R.; Nijem, N.; Li, K.; Li, J.; Chabal, Y. J.; Langreth, D. C. *Phys. Rev. B* **2009**, *79*, 081407(R).
(39) Moses, P. G.; Mortensen, J. J.; Lundqvist, B. I.; Nørskov, J. K. *J. Chem. Phys.*, in press.
(40) Langreth, D. C.; et al. *J. Phys.: Condens. Matter* **2009**, *21*, 084203.
(41) French, R. H. *Rev. Mod. Phys.* To be published.
(42) Cooper, V. R.; Thonhauser, T.; Puzder, A.; Schröder, E.; Lundqvist, B. I.; Langreth, D. C. *J. Am. Chem. Soc.* **2008**, *130*, 1304.
(43) Cooper, V. R.; Thonhauser, T.; Langreth, D. C. *J. Chem. Phys.* **2008**, *128*, 204102.
(44) Jurecka, P.; Sponer, J.; Hobza, P. *Phys. Chem. Chem. Phys.* **2006**, *8*, 1985.
(45) Stiborová, M.; Bieler, C. A.; Wiessler, M.; Frei, E. *Biochem. Pharmacol.* **2001**, *62*, 1675.
(46) Perdew, J. P.; Burke, K.; Ernzerhof, M. *Phys. Rev. Lett.* **1996**, *77*, 3865.
(47) Zhang, Y.; Yang, W. *Phys. Rev. Lett.* **1998**, *80*, 890.
(48) Chelikowsky, J. R.; Troullier, N.; Saad, Y. *Phys. Rev. Lett.* **1994**, *72*, 1240; see http://www.ices.utexas.edu/parsec/.
(49) Troullier, N.; Martins, J. L. *Phys. Rev. B* **1991**, *43*, 1993.
(50) Berman, H. M.; Olson, W. K.; Beveridge, D. L.; Westbrook, J.; Gelbin, A.; Demeny, T.; Hsieh, S. H.; Srinivasan, A. R.; Schneider, B. *Biophys. J.* **1992**, *63*, 751–759; see http://ndbserver.rutgers.edu/.
(51) Olson, W. K.; et al. *J. Mol. Biol.* **2001**, *313*, 229.
(52) The CG:CG minimum here is at an angle somewhat too small. Cooper et al.[42] attribute this to the fact that Roll and Propeller, known to be significant in this step, were not included in the calculation.

JP905765C